The Astronomical Journal, 139:1983–1992, 2010 May doi:10.1088/0004-6256/139/5/1983

SIMULTANEOUS *K*- AND *L*-BAND SPECTROSCOPY OF Be STARS: CIRCUMSTELLAR ENVELOPE PROPERTIES FROM HYDROGEN EMISSION LINES*

A. Granada[1,2], M. L. Arias[1,2], and L. S. Cidale[1,2]

[1] Facultad de Ciencias Astronómicas y Geofísicas, Universidad Nacional de La Plata, Paseo del Bosque S/N, La Plata, Buenos Aires, Argentina; granada@fcaglp.unlp.edu.ar

[2] Instituto de Astrofísica de La Plata (CCT La Plata-CONICET, UNLP), Paseo del Bosque S/N, La Plata, Buenos Aires, Argentina

Received 2009 November 20; accepted 2010 February 17; published 2010 April 8

ABSTRACT

We present medium-resolution *K*- and *L*-band spectra of a sample of eight Be stars, obtained with Gemini/NIRI. The IR *K* and *L* bands contain many lines of different hydrogen series that are used as a diagnosis to the physical conditions in the circumstellar environments. We make an analysis on the optical depths of the line-forming regions based on the intensity ratios of Pfγ and Brα lines, the behavior of Humphreys' series, and the fluxes of Brα and Brγ lines. All our targets show spectroscopic and photometric long-term variability; thus, time-resolved *K*- and *L*-band spectroscopy is an ideal tool for studying the structure and evolution of the innermost regions of the envelope and to test models on the disk-forming mechanism. We note that the instrumental configuration used allowed us to obtain good quality IR observations and to take profit of Gemini band 3 observing time (allocation time for ranked programs in which the observing conditions are relaxed).

Key words: circumstellar matter – line: formation – stars: activity – techniques: spectroscopic

1. INTRODUCTION

Classical Be stars are rapidly rotating non-supergiant B-type stars which have shown, at least once, Hα in emission (Jaschek & Jaschek 1987). Be stars also have moderate IR excesses (Waters et al. 1987; Dougherty et al. 1994), and their IR spectra are dominated by hydrogen emission lines (Lenorzer et al. 2002b), which suggest the presence of dense gaseous circumstellar envelopes, mostly compatible with a disk geometry. Another defining characteristic of Be stars is their spectroscopic and photometric variability on different timescales, from hours to decades, attributed to diverse phenomena, such as binarity, non-radial pulsations, magnetic fields, and mass ejections. In particular, the long-term spectrophotometric variability is commonly associated with discrete mass-loss episodes and reveals significant structural changes in the circumstellar environment (e.g., Štefl et al. 2003; Reig et al. 2005).

While far-UV lines of highly ionized elements form in hot regions close to the stellar photosphere, optical hydrogen lines are affected by the extended parts of the circumstellar envelope; in particular, the near-IR hydrogen lines probe an intermediate region of the envelope. Because of the small contribution of the photospheric absorption to hydrogen IR line profiles, the study of IR spectral regions in Be stars permits us to infer physical properties, morphology, and dynamics of the circumstellar envelopes (Lenorzer et al. 2002a), which cannot easily be acquired from other spectral regions.

The determination of parameters such as density and temperature gradients in the circumstellar medium is useful to set constraints on the theoretical models of the Be phenomenon. Moreover, an IR classification scheme of classical Be stars could be used in those cases in which it is not possible to perform the optical standard classification (Hanson et al. 1996); in the near IR, the interstellar absorption is 80 times less than that in the optical (Rieke & Lebofsky 1985).

Most of the spectroscopic studies of Be stars in the near-infrared region cover the *H* and/or *K* bands (Ashok & Banerjee 2000; Clark & Steele 2000; Steele & Clark 2001; Hanson et al. 1996; Lenorzer et al. 2002b) and are mainly devoted to spectral classification. Even though it presents numerous hydrogen lines of different series, the *L* band has been less explored (Lenorzer et al. 2002b; Mennickent et al. 2009).

We present in this work new IR spectra of a group of Be stars that were observed simultaneously in both *K* and *L* bands. The selected targets are widely studied in the UV and optical range (e.g., Floquet et al. 2000, 2002; Tubbesing et al. 2000; Arias et al. 2004; Granada & Cidale 2006; Hirata 1995) and are highly variable objects. We seek to derive the physical conditions of their circumstellar envelopes by a thorough analysis of their H recombination lines. Moreover, this work sets up a starting point of a campaign to follow up some of our targets in the IR region. Time-resolved IR observations of these Be stars would provide clues on the formation mechanism and the structure of their circumstellar environments.

2. OBSERVATIONS AND DATA REDUCTION

We obtained simultaneous *L*- and *K*-band spectra of a sample of eight Be stars with the Near InfraRed Imager and Spectrometer (NIRI) at the Gemini Observatory in Mauna Kea, Hawaii. We chose a queue mode observation, which offers the potential of better matching observations to the prevailing conditions (e.g., image quality, sky background, cloud cover). The queue programs can be assigned one of the three science ranking bands. Gemini's goal is to observe the entire allocated time of all programs in ranking bands 1 and 2, and to make every effort to complete as many band 3 programs as possible. Every night, several factors combine to determine which program is executed from the pool of possible queue observations. Scientific ranking is prioritized, as well as closeness of the current observing conditions to those required by the principal investigator

* Based on observations obtained at the Gemini Observatory, which is operated by the Association of Universities for Research in Astronomy, Inc., under a cooperative agreement with the NSF on behalf of the Gemini partnership: the National Science Foundation (USA), the Science and Technology Facilities Council (UK), the National Research Council (Canada), CONICYT (Chile), the Australian Research Council (Australia), Ministério da Ciência e Tecnologia (Brazil), and Ministerio de Ciencia, Tecnología e Innovación Productiva (Argentina).

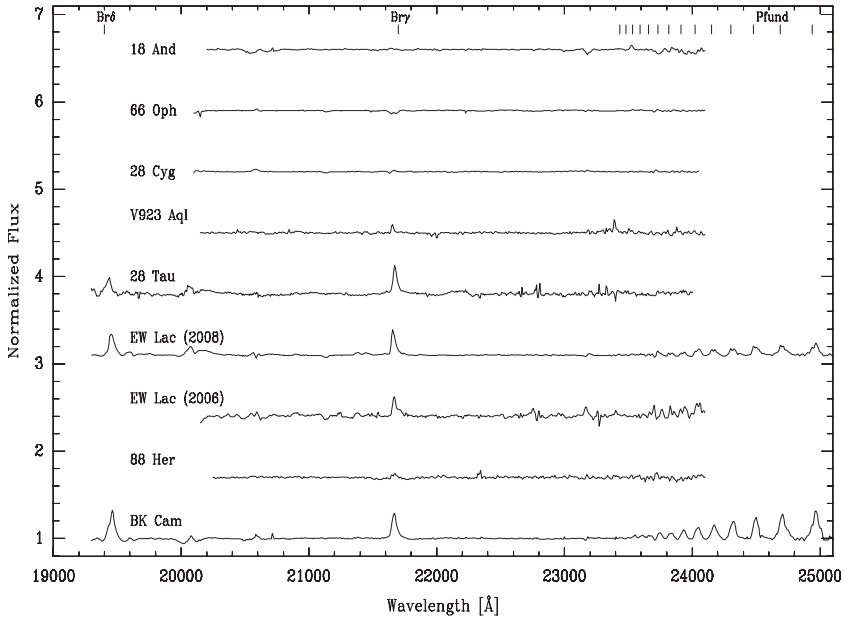

Figure 1. *K*-band spectra of our sample of eight Be Stars. The positions of hydrogen lines are indicated in the top part of the figure.

Table 1
Our Be Star Sample in the *K* and *L* Bands with Gemini/NIRI[a]

Object	HD	S.T.	Group	$V \sin i$ (km s^{-1})	Binary	Date (yyyy/mm/dd)
BK Cam	20336	B2.5 Ve	I	328 ± 21(a)	Yes	2008/11/25
28 Tau	23862	B8 IVev	II	286 ± 16(a)	Yes	2006/08/20
88 Her	162732	Bp she	I	310 ± 16(a)	Yes	2006/08/21
66 Oph	164284	B2 Ve	II	280 ± 17(a)	Yes	2008/08/25
V923 Aql	183656	Bp she	II	270 ± 20(a)	Yes	2006/09/17
28 Cyg	191610	B2.5 Ve	II	300 ± 20(a)	···	2008/08/25
EW Lac	217050	B3 IVshe	II	340 ± 22(a)	?	2006/08/20
						2008/09/09
18 And	222304	B9 V	III?	188(b)	···	2008/09/09

Notes. [a] The classification of the stars in the different groups is defined in Section 3.1.
References: (a) Fremat et al. 2005; (b) Royer et al. 2007.

(PI). In order to improve the chances of having a band 3 program executed, the PI is asked to relax the default observing conditions and modify the observing strategy.

Our observations were performed in two different observing campaigns during the nights of 2006 August 20–21 and September 17 (in Gemini band 2), and 2008 August 25, September 9 and November 25 (in Gemini band 3). The $f/6$ camera with the 2 pixel slit was used to obtain a resolving power of 1300 and 1100 in the *K* and *L* bands, respectively. The spectra were reduced by using the Gemini tasks of the IRAF[3] packages. We performed the telluric and instrument correction by taking the ratio of the program object spectrum with that of a late B telluric standard observed near the object in both time and sky position (air mass).

We selected late B standards because the only intrinsic features they exhibit are neutral hydrogen lines. Once the stellar H lines were removed from these standard stars, the program star fluxes were divided by the fluxes of their corresponding calibrators, canceling out the effect of telluric features, atmospheric extinction, and instrumental effects. Finally, the resultant spectra were multiplied by an adequate blackbody distribution, according to the effective temperature of the telluric standard star. It is worth noting that flux calibration is inaccurate because of slit losses, which vary somewhat with wavelength (due to differential refraction and the wavelength dependence of seeing). For this reason, spectrophotometric standards are not done as part of the standard baseline calibration. The accuracy for which the relative flux density of a telluric standard is known is probably better than 10% for a given atmospheric window (http://www.gemini.edu/sciops/instruments/niri/calibration).

Following the above-described procedure, the telluric bands were successfully removed from our spectra, except in the wavelength shortward of 3.4 μm in the *L* band and around 2.0 μm in the *K* band, where heavy and variable atmospheric absorption were impossible to remove. The observing log is given in Table 1, together with the date of observation and some other characteristics of the objects that will be commented throughout the following section. The continuum normalized spectra in the *K* and *L* bands of our eight Be stars are shown in Figures 1 and 2.

2.1. The Stellar Sample

In this subsection, we comment on the spectrophotometric variability of our targets. In particular, we describe the long-term behavior of the Hα line profile, based on data

[3] IRAF is distributed by the National Optical Astronomy Observatory, which is operated by the Association of Universities for Research in Astronomy (AURA) under cooperative agreement with the National Science Foundation.

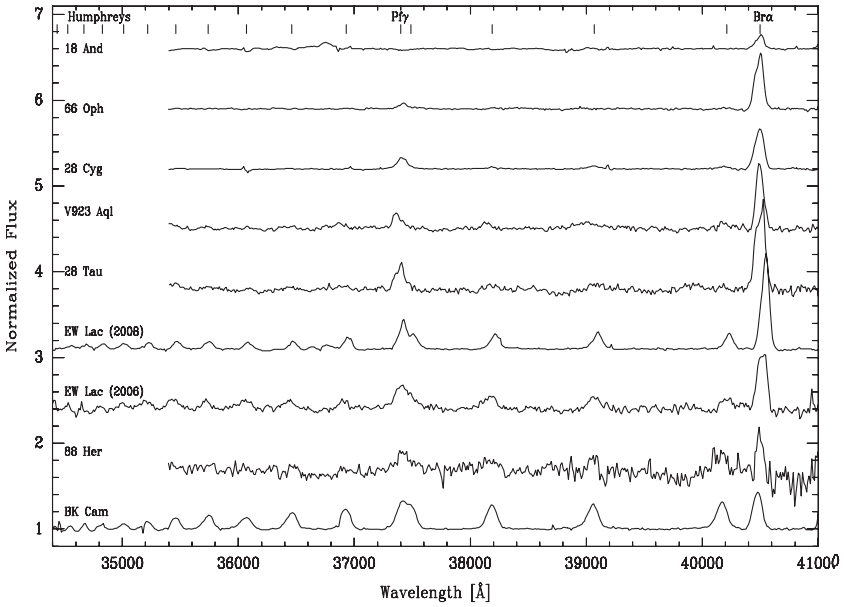

Figure 2. *L*-band spectra of our sample of eight Be stars. The positions of hydrogen lines are indicated in the top part of the figure.

obtained from the literature and the Be star spectra database (http://basebe.obspm.fr/basebe/).

1. EW Lac is an early-type shell star (Slettebak 1982) which has been observed since 1882 presenting spectral and photometric variability in different timescales: a 0.7 day photometric variability of 0.2 mag was reported by Walker (1958), Pavlovski et al. (1993) reported multiperiodicity in this object, and Jeong et al. (1986) found photometric variations of 50–60 days. Percy et al. (1996) determined a 3000 day photometric period. From radial velocity measurements, Antonello et al. (1982) proposed that EW Lac could be a 40.3 year binary system. The Hα profile exhibited a roughly constant maximum intensity with an increasing central absorption from 1999 to 2001. Since then the emission has slightly strengthened, and strong changes in the V/R ratio have occurred.
2. 28 Cyg is an early-type Be star. It shows short-term photometric variations on a timescale of about a day (Percy & Bakos 2001). Peters & Penrod (1988) confirmed conspicuous mass-loss activity and moving structures in the optical line profiles. Tubbesing et al. (2000) found a possible connection between the outbursts in this star and beating between two short-term periods. During the last 10 years, Hα has been observed in emission, showing two peaks. Since 2005, the photospheric component of Hα has become increasingly visible, even dominating the line profile by mid 2009.
3. 66 Oph is a highly variable early-type object in both light and Hα emission intensity (Floquet et al. 2002). IUE observations revealed the presence of recurrent mass-loss rates taking place every year (Grady et al. 1987; Peters 1988, 2000). This star is known to be a multiple system with a close binary orbiting the primary Be star (Štefl et al. 2004). The system has been recently resolved by speckle interferometry (Mason et al. 2009). Regarding Hα, this object exhibited a profile in pure emission, with a normalized intensity larger than 8, in 1993. Since then, the line has faded. During 2009 September, the star shows its photospheric absorption, with central emission similar to that of 28 Cyg.
4. BK Cam is an early-type emission-line star. McLaughlin (1963) suggested the possibility of this star being a close system, and recently it has been resolved by speckle interferometry (Mason et al. 2009). BK Cam displayed spectroscopic variability with a period of around 4.5 years, before entering an inactive stage from 1938 to 1961. From 1999 to 2002, the Hα profile had a maximum intensity between 1.8 and 1.9, with V/R variations and central absorption reaching the intensity 1.7. Since 2003, the line has strengthened significantly, reaching an intensity of 3 in the red peak by 2009 September.
5. 28 Tau is a late-type spectroscopic binary, with an orbital period of 218 days (Katahira et al. 1996). Recent speckle interferometry could not resolve the two components (Mason et al. 2009). The null companion detection could probably be due to the large Δm of the observed pair (see Figure 1 of Mason et al. 2009).

   Hirata (1995) made an interesting review of the long-term variability of this star: during the past 100 years, it has gone through B, Be shell, and Be phases, and also through photometric variations, with a period of 34 years (see Sadakane et al. 2005, and references therein). The last activity cycle or disk development started in 1972; thus our 2006 observations of Pleione were obtained close to the development of a new disk. Taranova et al. (2008) reported on the fading of Pleione in the near infrared (1.25–3.5 μm) in 1999–2007. Tanaka et al. (2007) found remarkable changes in both the brightness and the profiles of the Balmer and metallic lines, during 2005 November and 2007 April. In 1990, the two-peak Hα line was weak. Since then, it strengthened until 1996, when a single peak of intensity around 6 was observed. In 1999, the emission weakened, reaching a value of 4, and by the end of the year it recovered its previous intensity. The observations of 2001 allowed us to resolve two emission peaks with intensity larger than 5; during 2002, the blue peak was more intense than the red peak, and from 2002 to 2007 the line faded. By the end of 2007, the Hα line started strengthening, in coincidence with the beginning of a long-term cycle. Polarimetric observations revealed variations

of the intrinsic polarization angle from 60° to 130° in 1974–2003. Variations in both Hα and the polarization angle are indicative of the spatial motion of the disk axis supporting the hypothesis of a precessing disk outside the equatorial plane (Hummel 1998; Hirata 2007).

6. 88 Her is a late Be/shell star. It is a spectroscopic binary, with an orbital period of 86.7 days (Harmanec et al. 1972). Doazan et al. (1982) found that the Hα V/R variations follow the binary period in spite of the large long-term changes in the intensity of the emission line. The star also presents long-term *UVB* variations similar to those of Pleione with a period of around 10 years. From 1996 to 2002, Hα weakened, displaying V/R variations and strong central absorption. Since 2002, the emission peaks of this shell line have increased.
7. V923 Aql is a late-type Be-shell star. This star exhibits spectroscopic and photometric variations of different timescales: Merrill (1952) proposed a 6.5 year period from radial velocity measurements; Lynds (1960) reported variations with a period shorter than one day; Koubský et al. (1989) proposed that the variation of the radial velocities came from the superposition of cyclic long-term variations with variable amplitude ($P \sim$ 1800–2400 days) and the orbital movement ($P = 214.75$ days). These authors concluded that the binary system was composed by a B5–7 primary star and a low-mass component of about 0.5 $M_{\odot}$, and derived several sets of orbital parameters. Mennickent et al. (1994) found a quasi-period of 7 years and an amplitude of 0.25 mag in the *U* band. Pavlovski et al. (1997) found significant variations in the light curve and *color*. Arias et al. (2004) found variations in the intensity of Fe II lines correlated with the orbital period of 214.75 days, and determined a period of 6.8 years to the V/R variations of the Hα line. The Hα shell line has varied in intensity and V/R ratio from 1999 to the present.
8. 18 And is a B9Ve star. We selected it as the telluric standard for EW Lac because it figured as a B9V star in several catalogs and was close to our target. However, it turned out to show the Brα line in emission, and when looking for previous data, we found a paper of Coté & van Kerkwijk (1993) showing Hα emission in this object. Hα has been observed in the last years showing strong photospheric absorption with two central emission peaks which do not reach the continuum.

3. RESULTS

The *K* band, centered in 2.2 μm, displays Brγ and Brδ as well as many lines of the higher members of the Pfund series; see Figure 1. In all our Be stars, Brγ is in emission or filling the photospheric absorption. Brδ and Pfund lines fall at the limits of the spectral range of the *K* band and thus could only be measured in those spectra with the best signal-to-noise ratio. In these cases, the lines appear in emission.

In the stars with the earliest spectral types (66 Oph, BK Cam, EW Lac and 28 Cyg), He I lines can be found. The presence of the He I 2.058 μm feature in emission evidences a large *ionizing* flux and a dense circumstellar environment. The He I 2.112 μm line is in absorption in all our early-type objects, and the He I 2.161 μm feature is in emission but blended with Brγ.

In EW Lac, BK Cam, and 66 Oph, weak emission lines of the Mg II 2.138, 2.144 μm doublet are evident but their equivalent widths, *W*, could not be measured accurately. Even though in all cases $W_{2.138} > W_{2.144}$, the line ratios do not seem to satisfy the relation $W_{2.138}/W_{2.144} \sim 2$, which is expected when both transitions are optically thin (see Clark & Steele 2000, and references therein).

The Fe II 2.089 μm line is only observed in EW Lac. This emission line is characteristic of moderately warm and dense environments (Hamann & Simon 1987).

For the Be stars of later spectral types, the only near-IR features in the *K* band are hydrogen emission lines.

The *L* band, around 3.5 μm, displays only hydrogen lines (see Figure 2) as well. In all our targets, Brα and Pfγ lines appear in emission. The exception is 18 And for which the only emission feature is Brα. For some stars, Humphreys' lines, from the transition 6–14 up to 6–27, are also observed in emission.

We have measured line fluxes (Fl), equivalent widths (*W*) and FWHM of the hydrogen lines using IRAF tasks. The equivalent widths of Brackett and Pfund lines were corrected taking into account the photospheric absorption component corresponding to the underlying star. A correction for photospheric absorption of the equivalent widths is not required in Humphreys' lines, because normal B-type stars do not exhibit evident Humphreys' absorption profiles (Lenorzer et al. 2002b). Tables 2 and 3 show the corrected equivalent widths and fluxes, respectively. 18 And has been excluded from the forthcoming analysis because its only emission features are Brα and a weak Brγ.

The FWHMs were corrected for the instrumental width (Fekel 1997), which is $\sim$230 km s^{-1} in the *K* band and $\sim$270 km s^{-1} in the *L* band. The calculated values are listed in Table 4. In most cases, these large values prevent us from resolving two-peaked lines, except for the Pfund lines in the *K* band for EW Lac where two-peaked profiles are evident.

We estimate an error in our measurements of about 10% for the line fluxes and equivalent widths, and of 40 km s^{-1} for the FWHM. The accuracy of our measurements is mainly limited by the instrumental resolution, the signal-to-noise ratio of the spectra, the determination of the continuum level, and the inexact correction for the atmospheric absorption.

3.1. The Behavior of the Equivalent Widths and Flux Ratios of IR Lines in K and L Bands

According to the intensity of the *L*-band hydrogen emission lines, Be stars can be classified in three groups following the scheme by Mennickent et al. (2009): group I contains the stars with Brα and Pfγ equally intense as Humphreys' lines, group II consists of those stars with Brα and Pfγ more intense than Humphreys' lines, and group III is made up of those where no emission is detected (Figure 2). A simple inspection of our spectra allowed us to classify most of the stars as belonging to group II, with the exception of 88 Her and BK Cam which belong to group I, and 18 And which was classified as a group III object (see Table 1). It is worth noting that 66 Oph does not exhibit emission in the Humphreys series, being an extreme group II member.

In order to study the optical depth of the IR line-forming regions of stars in groups I and II, we analyze the behavior of hydrogen equivalent widths and line flux ratios.

Figure 3 (left) shows the position of our targets in the Lenorzer et al. (2002a) *L*-band line flux ratios diagram. The location of a star in this plot reveals information on the optical thickness of the forming region of Brα, Pfγ, and Hu$_{6-14}$ lines. Group I objects (BK Cam and 88 Her) are located on the top right part of the diagram, indicating that the lines might form in an optically thick disk-like circumstellar envelope. Line ratios close to the Menzel case B recombination model (Baker & Menzel 1938;

Table 2
Equivalent Widths of Hydrogen Emission Lines in Our *K*- and *L*-band Spectra in Å, Corrected by Photospheric Absorption[a]

Line	λ(μm)	BK Cam	28 Tau	88 Her	66 Oph	V923 Aql	28 Cyg	EW Lac_{2006}	EW Lac_{2008}
H I $_{5-4}$	4.052	45.6	106.2	30.5	58.8	63.5	49	71	91
H I $_{14-6}$	4.021	30.4	11.0	20.0	···	5	4	13	15
H I $_{15-6}$	3.908	28.1	8.3	em	···	em	4	18	16
H I $_{16-6}$	3.820	26.3	6.7	em	···	em	2	20	17
H I $_{17-6}$	3.750	23.0	em	em	···	em	em	em	14
H I $_{8-5}$	3.741	34.0	35.4	21.9	9.9	16.3	17.9	33.9	32.9
H I $_{18-6}$	3.693	22.1	5.0	em	···	em	···	8	11
H I $_{19-6}$	3.646	19.4	4.2	em	···	···	···	11	7
H I $_{20-6}$	3.607	17.2	···	em	···	···	···	13	6
H I $_{21-6}$	3.574	15.2	···	···	···	···	···	9	6
H I $_{22-6}$	3.546	11.0	···	···	···	···	···	13	6
H I $_{23-6}$	3.522	9.0	···	···	···	···	···	10	5
H I $_{24-6}$	3.501	5.4	···	···	···	···	···	5	5
H I $_{25-6}$	3.483	3.4	···	···	···	···	···	em	4
H I $_{26-6}$	3.467	···	···	···	···	···	···	em	em
H I $_{27-6}$	3.452	···	···	···	···	···	···	em	em
H I $_{9-5}$	3.297	···	···	···	···	···	···	···	50.7
H I $_{10-5}$	3.040	26.6	18.0	···	···	···	···	10	30.2
H I $_{17-5}$	2.495	19.8	···	···	···	···	···	···	7.8
H I $_{18-5}$	2.470	17.84	···	···	···	···	···	···	7.3
H I $_{19-5}$	2.449	10.9	···	···	···	···	···	···	5.8
H I $_{20-5}$	2.431	10.4	···	···	···	···	···	···	4.1
H I $_{21-5}$	2.416	8.7	···	···	···	···	···	···	4.1
H I $_{22-5}$	2.404	6.8	···	···	···	···	···	6.1	3.9
H I $_{23-5}$	2.393	4.4	···	···	···	···	···	5.8	2.0
H I $_{24-5}$	2.383	3.4	···	···	···	···	···	5.0	1.7
H I $_{25-5}$	2.373	2.6	···	···	···	···	···	2.72	2.1
H I $_{26-5}$	2.366	em	···	···	···	···	···	em	em
H I $_{27-5}$	2.359	1.5	···	···	···	···	···	em	em
H I $_{28-5}$	2.353	em	···	···	···	···	···	em	em
H I $_{7-4}$	2.166	20.2	19.1	10.1	3.5	10.4	6.5	13.8	15.8
H I $_{8-4}$	1.940	21.1	18.4	···	···	···	···	···	16

Notes. [a] The estimated uncertainties in the *W* measurements are of 10%. Here positive values of *W* correspond to emission lines. Those lines where emission is evident but difficult to measure are indicated with *em*.

Osterbrock 1989 p.77) correspond to optically thin lines like forming in an isothermal stellar wind (bottom left part of the diagram). Group II stars spread over a region of moderate to small line optical depth.

Using the most intense lines of *K* and *L* bands, Brα, Brγ, and Pfγ, we build a line flux diagram similar to that of Persson & McGregor (1985) (Figure 3 (right)). Group I objects are located in the bottom left part of this diagram, while group II objects are in the middle part. Thus, these lines are also useful to discriminate between compact thick envelopes from extended thin ones.

The position of EW Lac in Figure 3 indicates that it could be a transition object between both groups. 28 Cyg shows similar behavior, in the sense that its location in the diagram changed significantly from the mid-90s (Lenorzer et al. 2002a), the open square in Figure 3 (left) to 2008 (this work), showing a clear transition from group I to group II. These results may be interpreted in terms of the ejection of an optically thick envelope, at the IR line frequencies, that expands and becomes optically thin in 2008 (Mennickent et al. 2009; de Wit et al. 2006). The contemporaneous fading observed in Hα is consistent with this scenario.

In Figure 4, we plot the flux ratios of each Humphrey's line, Hu_{6-n} to Hu_{6-19} versus wavelength for EW Lac and BK Cam, for which Humphreys' series (from transition 6–14 to 6–25) was measured most accurately. We find that at a certain value of λ, characteristic of each object, Humphreys' lines of these stars deviate from the relation defined by optically thin lines (solid line).

For those Humphreys' lines with fluxes that deviate from the ones corresponding to the optically thin case, rough estimates of the atom column density and the extension of the line-forming regions can be made. The emitted flux of Humphreys' lines can be written as

$$\mathrm{Fl}_{\mathrm{Hu}_n} = \mathrm{Fl}_{\mathrm{Hu}_{n\,\mathrm{thin}}} e^{-\tau},$$

where *n* is the quantum number of the upper level from which the transition line takes place, the subscript thin refers to optically thin lines, and τ represents the line optical depth:

$$\tau = \frac{\sqrt{\pi}\, e^2 f}{m_e\, c\, \Delta\nu_{\mathrm{D}}} N_i,$$

where N_i is the atom column density of the emitting material, f is the line oscillator strength, and $\Delta\nu_{\mathrm{D}}$ is the Doppler width of the line. Since the main line broadening mechanism is rotation, we adopt the value of $V \sin i$ for $\Delta\nu_{\mathrm{D}}$.

Then, the atom column density can be calculated from each line measurement as

$$N_i = \ln\left(\frac{\mathrm{Fl}_{\mathrm{Hu}_{n\,\mathrm{thin}}}}{\mathrm{Fl}_{\mathrm{Hu}_n}}\right) \frac{m_e\, c\, \Delta\nu_{\mathrm{D}}}{\sqrt{\pi}\, e^2 f}.$$

Table 3
Hydrogen Emission-line Fluxes, in Units of 10^{-13} erg cm^{-2} s^{-1} Å^{-1} [a]

Line	$\lambda(\mu m)$	BK Cam	28 Tau	88 Her	66 Oph	V923 Aql	28 Cyg	EW Lac_{2006}	EW Lac_{2008}
H I $_{5-4}$	4.052	12.01	7.01	0.60	19.60	10.22	13.1	2.97	34.00
H I $_{14-6}$	4.021	8.16	0.70	0.44	...	0.83	1.10	0.56	5.51
H I $_{15-6}$	3.908	7.99	0.59	...	...	...	1.22	0.84	5.58
H I $_{16-6}$	3.820	8.03	0.52	...	...	...	0.72	1.02	5.98
H I $_{17-6}$	3.750	7.41	...	...	...	...	...	...	6.27
H I $_{8-5}$	3.741	11.10	4.21	0.88	4.44	3.43	6.19	1.83	15.2
H I $_{18-6}$	3.693	7.50	0.44	...	...	...	...	0.47	5.23
H I $_{19-6}$	3.646	6.88	0.39	...	...	...	...	0.66	4.43
H I $_{20-6}$	3.607	6.35	...	...	...	...	...	0.82	3.03
H I $_{21-6}$	3.574	5.87	...	...	...	...	...	0.59	3.13
H I $_{22-6}$	3.546	4.35	...	...	...	...	...	0.87	3.16
H I $_{23-6}$	3.522	3.68	...	...	...	...	...	0.69	2.70
H I $_{24-6}$	3.501	2.23	...	...	...	...	...	0.35	2.75
H I $_{25-6}$	3.483	1.17	...	...	...	...	...	...	2.24
H I $_{9-5}$	3.297	...	...	...	...	...	...	...	41.2
H I $_{10-5}$	3.040	16.87	3.45	...	...	...	...	1.92	32.4
H I $_{17-5}$	2.495	14.27	...	...	...	...	...	...	32.4
H I $_{18-5}$	2.470	13.39	...	...	...	...	...	...	7.05
H I $_{19-5}$	2.449	8.61	...	...	...	...	...	...	6.80
H I $_{20-5}$	2.431	8.56	...	...	...	...	...	...	5.60
H I $_{21-5}$	2.416	7.43	...	...	...	...	...	...	4.07
H I $_{22-5}$	2.404	6.00	...	...	...	...	...	5.60	4.13
H I $_{23-5}$	2.393	3.92	...	...	...	...	...	5.41	4.06
H I $_{24-5}$	2.383	3.15	...	...	...	...	...	4.72	2.11
H I $_{25-5}$	2.373	2.39	...	...	...	...	...	2.61	2.28
H I $_{27-5}$	2.359	1.43	...	...	...	...	...	...	...
H I $_{7-4}$	2.166	26.26	13.05	3.91	2.12	8.87	10.4	18.6	23.3
H I $_{8-4}$	1.940	38.49	19.16	...	...	...	...	...	33.9

Note. [a] The estimated uncertaintes in the line flux measurements are of 10%.

Table 4
Corrected FWHM, in km s^{-1} [a]

Line	$\lambda(\mu m)$	BK Cam	28 Tau	88 Her	66 Oph	V923 Aql	28 Cyg	EW Lac_{2006}	EW Lac_{2008}
H I $_{5-4}$	4.052	633	766	...	551	475	617	640	517
H I $_{14-6}$	4.021	687	...	...	598	419	750	752	538
H I $_{15-6}$	3.908	735	...	...	...	...	855	783	634
H I $_{16-6}$	3.820	712	...	...	...	523	...	935	617
H I $_{17-6}$	3.750	683	...	...	...	...	...	...	479
H I $_{8-5}$	3.741	711	754	518	444	651	830	774	544
H I $_{18-6}$	3.693	661	...	...	...	...	...	591	544
H I $_{19-6}$	3.646	785	...	...	...	...	...	889	562
H I $_{20-6}$	3.607	794	...	...	...	...	...	...	588
H I $_{21-6}$	3.574	704	...	...	...	...	...	632	604
H I $_{22-6}$	3.546	619	...	...	...	...	...	854	582
H I $_{23-6}$	3.522	726	...	...	...	...	...	879	539
H I $_{24-6}$	3.501	601	...	...	...	...	...	...	543
H I $_{25-6}$	3.483	...	...	...	...	...	...	...	469
H I $_{9-5}$	3.297	...	...	...	...	...	...	...	...
H I $_{10-5}$	3.040	624	646	...	...	...	...	...	...
H I $_{16-5}$	2.526	...	...	...	...	...	...	...	521
H I $_{17-5}$	2.495	677	...	...	...	...	...	...	670
H I $_{18-5}$	2.470	727	...	...	...	...	...	...	766
H I $_{19-5}$	2.449	481	...	...	...	...	...	...	659
H I $_{20-5}$	2.431	518	...	...	...	...	...	...	607
H I $_{21-5}$	2.416	633	...	...	...	...	...	...	706
H I $_{22-5}$	2.404	557	...	...	...	...	...	...	597
H I $_{23-5}$	2.393	440	...	...	...	...	...	...	556
H I $_{24-5}$	2.383	498	...	...	...	...	...	...	650
H I $_{25-5}$	2.373	358	...	...	...	...	...	...	433
H I $_{27-5}$	2.359	...	...	...	...	...	...	...	...
H I $_{7-4}$	2.166	579	416	...	...	em	sh	255	410
H I $_{8-4}$	1.940	795	...	...	...	...	...	...	735

Note. [a] The uncertaintes in the FWHM measurements are of 40 km s^{-1}.

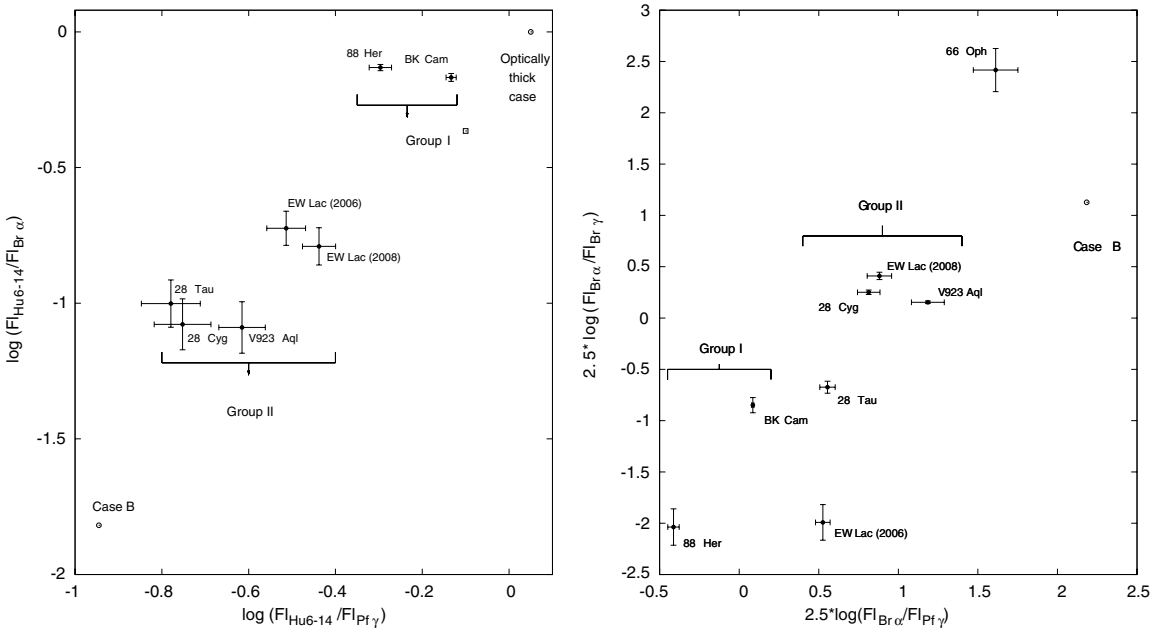

Figure 3. Left: line flux ratio diagram, similar to that of Lenorzer et al. (2002a). The open square indicates the position of 28 Cyg during the 1990s. Right: line flux ratio diagram similar to that of Persson & McGregor (1985).

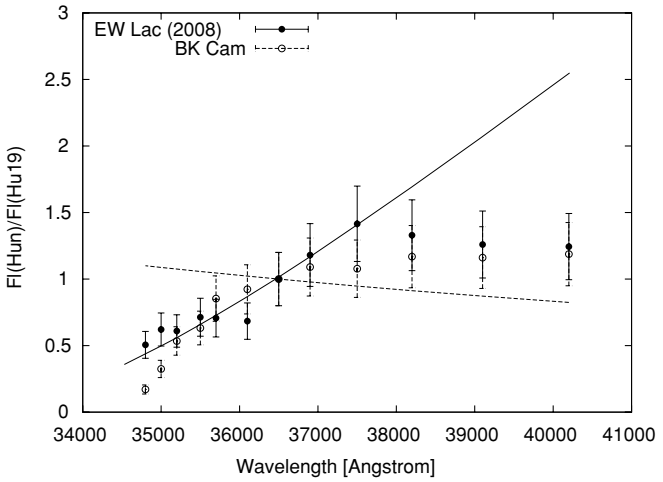

Figure 4. Behavior of the line flux ratios of Humphreys' lines. The continuous line corresponds to the optically thin case, while the dashed line represents the optically thick case.

Zorec et al. (2007) predict a smooth variation of the density with the distance in the inner regions of the circumstellar envelope of Be stars, of the form

$$\rho = \rho_o \left(\frac{R}{R_\star}\right)^{-0.5}.$$

As Humphreys' lines are supposed to form very close to the central star, we can simply approximate the mass density (and also the number density n_i) to a constant value all over the forming region. Thus, the atom column density can be rewritten as

$$N_i = \int_{R_{\rm int}}^{R_{\rm ext}} n_i(r)\, dr = \bar{n_i}\, \Delta R,$$

where $\Delta R = R_{\rm ext} - R_{\rm int}$.

Table 5
Column Densities and Relative Extensions of Humphreys' Line-forming Regions for BK Cam and EW Lac

	BK Cam		EW Lac	
Line	$N_i[\frac{10^{14}}{\rm cm^2}]$	$\frac{\Delta R_{{\rm Hu}\,n}}{\Delta R_{\rm Hu\,16}}$	$N_i[\frac{10^{14}}{\rm cm^2}]$	$\frac{\Delta R_{{\rm Hu}\,n}}{\Delta R_{\rm Hu\,16}}$
Hu_{14}	5.710	1.196	5.558	1.730
Hu_{15}	5.882	1.197	5.233	1.583
Hu_{16}	5.026	1.000	3.382	1.000
Hu_{17}	4.644	0.907	...	...
Hu_{18}	1.737	0.334	...	...

Since $\bar{n_i}$ is the same for all Humphreys' lines, it is possible to estimate the extension of Humphreys' line-forming regions relative to the extension of one of them:

$$\frac{N_{i\,{\rm Hu}\,n}}{N_{i\,{\rm Hu}\,16}} = \frac{\Delta R_{{\rm Hu}\,n}}{\Delta R_{{\rm Hu}\,16}},$$

and thus

$$\frac{\Delta R_{{\rm Hu}\,n}}{\Delta R_{{\rm Hu}\,16}} = \ln\left(\frac{{\rm Fl}_{{\rm Hu}_n\,{\rm thin}}}{{\rm Fl}_{{\rm Hu}_n}}\right)\left[\ln\left(\frac{{\rm Fl}_{{\rm Hu}_{16}\,{\rm thin}}}{{\rm Fl}_{{\rm Hu}_{16}}}\right)\right]^{-1}.$$

These results are shown in Table 5 where we list the values of the atom column densities and the extension of the optically thick line-forming region relative to the line Hu_{16} for BK Cam and EW Lac. We estimate that the uncertainty in the determination of N_i is approximately 40% and for the relative extension is of about 20%, since it can be calculated using only line flux ratios. We can see that for both stars the atom column densities are of the same order, about 10^{14} cm^{-2}, while the relative extension is rather larger in EW Lac than in BK Cam. This result suggests that the latter has a more compact Humphreys' line-forming region than the former, which is in agreement with the expected envelope properties for group II and group I stars, respectively.

Also, only these two objects allowed the measurement of Pfund lines in *K* and *L* bands. In these stars, the lines follow

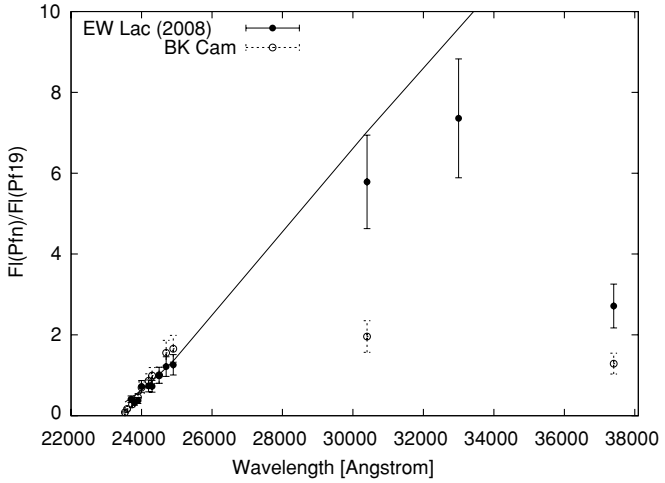

Figure 5. Behavior of the line flux ratios of Pfund lines. The continuous line corresponds to the optically thin case. The departure from the optically thin case of BK Cam is remarkable.

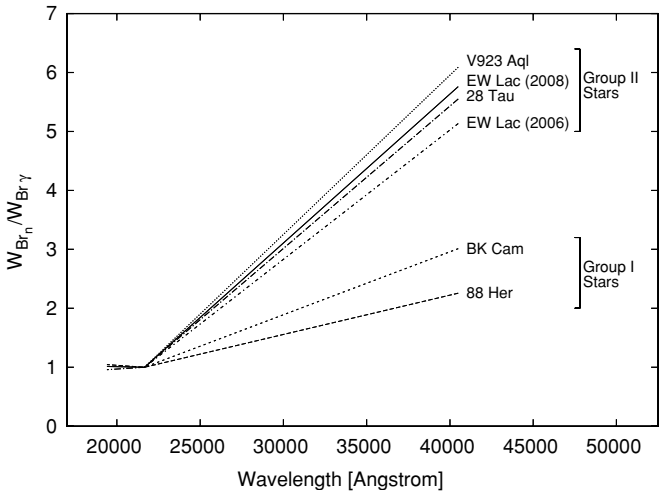

Figure 6. Behavior of the equivalent widths of the Brackett lines of K and L bands. For each star, the ratios of $W_{\mathrm{Br}\alpha}/W_{\mathrm{Br}\gamma}$, $W_{\mathrm{Br}\gamma}/W_{\mathrm{Br}\gamma}=1$, and $W_{\mathrm{Br}\delta}/W_{\mathrm{Br}\gamma}$ are joined with lines to highlight the slope in each case. There exists a clear difference in the slope of the Brackett series for group I and group II stars.

the optically thin relation for line transitions originating in the higher terms of the series but the behavior of Pfγ and Pfδ lines evidence a departure form the optically thin case (see Figure 5).

The observed departure from the optically thin case for lines arising from the lower members of both Humphreys' and Pfund's series suggests the existence of optical depth effects. However, effects such as disk or envelope truncation or different geometries could also influence on this departure.

We have found that stars belonging to group I display similar equivalent widths in Brα and Brγ lines, while in stars of group II the equivalent width of Brα is much larger than the equivalent width of the Brγ line, as shown in Figure 6. In the three stars, in which Brδ could be measured (28 Tau, BK Cam and EW Lac) the ratio $W_{\mathrm{Br}\delta}/W_{\mathrm{Br}\gamma}$ remained almost constant, suggesting that this quantity does not change much from one group to the other. If the stars moved from one group to the other, a change in the $W_{\mathrm{Br}\alpha}/W_{\mathrm{Br}\gamma}$ would be expected. This actually occurs for EW Lac, which displayed a strengthening in Brα, while the Brγ line hardly changed between 2006 and 2008.

In the two objects of group I, we have found that the line flux of Brα is smaller than the line flux of Brγ. This behavior

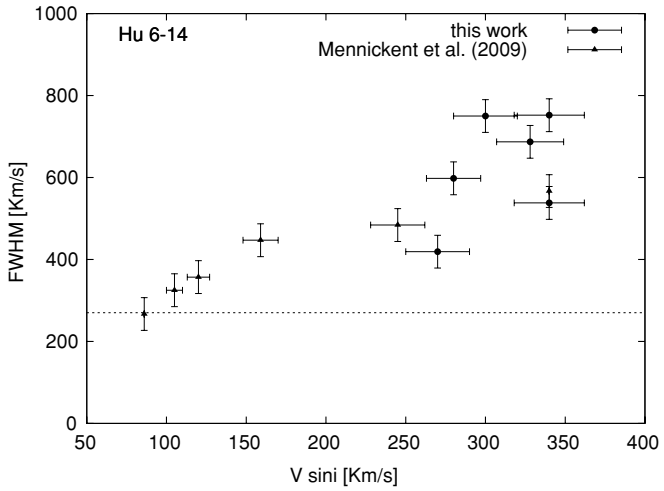

Figure 7. FWHM as a function of $V \sin i$ for Hu_{6-14}. The horizontal line represents the instrumental width.

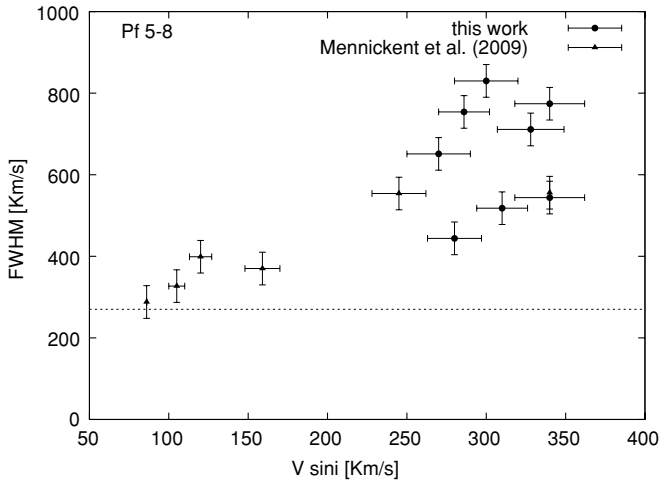

Figure 8. FWHM as a function of $V \sin i$ for Pfγ. The horizontal line represents the instrumental width.

is characteristic of the optically thick line models presented by Lynch et al. (2000), where a strong depression in the emission of Brα is predicted. The above analysis indicates that the material surrounding group I stars is optically thick to the Brackett lines in both K and L bands during the span of our observations. Such line optical depth effects have already been observed in the Be star δ Sco, after its last periastron passage (Banerjee et al. 2001) and also during the early stages after nova outbursts (Ashok et al. 2006; Lynch et al. 2001).

3.2. Correlation of FWHM with V sin i

In Figures 7–9 we have plotted the corrected values of FWHM of Hu_{6-14}, Pfγ, and Brα versus $V \sin i$, respectively. In the case of Pfγ and Hu_{6-14}, we included the data published by Mennickent et al. (2009).

The strong correlation of IR lines FWHM with $V \sin i$ indicates that the origin of emission-line broadening is mainly rotational, similarly to what Hanuschik (1989) found for hydrogen lines in the optical range. However, we do not find in our sample targets a growth of FWHM for higher terms of the Humphreys or Pfund series as expected if the rotational velocity in the inner disk was higher than in the outer part (Hony et al. 2000; Mennickent et al. 2009).

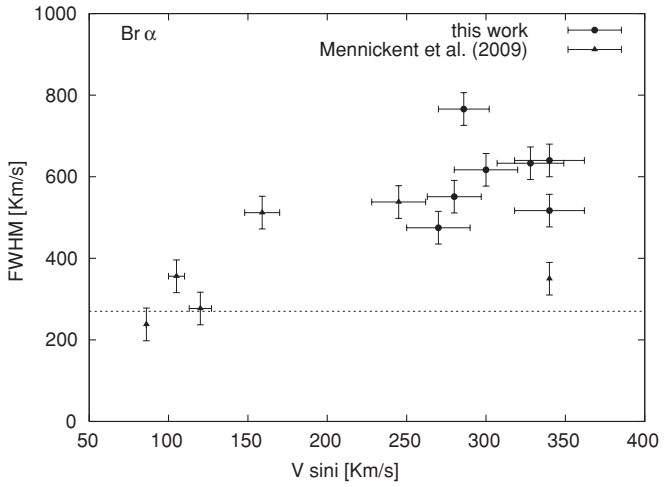

Figure 9. FWHM as a function of $V \sin i$ for Brα. The horizontal line represents the instrumental width.

4. DISCUSSION

The behavior of $\log(\mathrm{Hu}_{6-14}/\mathrm{Br}\alpha)$ versus $\log(\mathrm{Hu}_{6-14}/\mathrm{Pf}\gamma)$, as discussed in Lenorzer et al. (2002a) and Mennickent et al. (2009), allows us to investigate the nature of the circumstellar material surrounding Be stars and other objects with envelopes. Thus, IR hydrogen lines of group II stars presented in this work, 28 Tau, 66 Oph, V923 Aql, and 28 Cyg, would form in a region of moderate or small optical depth in the lines of Brackett, Pfund, and low transitions of Humphreys, whereas those of group I, 88 Her and BK Cam, could come from optically thick envelopes at IR line frequencies. EW Lac could be a transition object between these two groups.

All our objects have Hα observations (CASLEO,[4]) close to the epoch of the IR spectroscopy.

18 And is a poorly studied object. The spectra presented in this work are the first near-IR data reported for this star. Its only feature in the near IR is Brα in emission, but no Humphreys or Pfund emissions are evident. Its Hα quiescence as a weak shell line during the last decade indicates that no eruptive event has recently occurred.

In the case of 28 Tau, 66 Oph, and 28 Cyg, the observed Hα weakening is consistent with a dissipating disk during the epoch of our observations (e.g., Hirata 1995). At that time, the IR line emission of the mentioned stars was more likely to come from an optically thin wind/disk rather than from an optically thick disk. In the case of 28 Tau, after our 2006 near-IR spectroscopy, a new shell phase is characterized by an increase in the intensity of the emission peaks and a deepening of the central absorption of Hα started. This star is supposed to have started a new long-term cycle (Hirata 1995). Recent studies on the variations in both Hα and the polarization angle gave evidence of the spatial motion of the disk axis supporting the hypothesis of a precessing disk outside the equatorial plane (Hummel 1998; Hirata 2007). Thus, we consider that 28 Tau is an interesting object to follow up in the near IR.

For EW Lac we observe a noticeable increase in the Brα line intensity while lines from other series remained almost unchanged. Observations of Hα close to the epoch of our observations show that an increase in the emission occurred from 2006 to 2008 which could be related to an increase of the emitting surfaces of Brα and Hα lines.

[4] http://astrosurf.com/~buil/us/bestar.htm, http://basebe.obspm.fr

In the previous section we mentioned that our 2008 EW Lac spectrum exhibits double-peaked Pfund lines in the *K* band. The peak separation seems to increase toward the higher members of the series, which could indicate that the innermost regions of the envelope rotate faster (Huang 1972) and/or that scattering effects in the lines are relevant (Hummel & Dachs 1992; Hummel & Vrancken 2000). However, the scattering effects are more important in the lower members of the series (Hummel & Dachs 1992). As we have measured Pfund lines in the *K* band from Pf_{5-16} to Pf_{5-27}, we could make a rough estimation of the extension of the line-forming region, assuming that the separation of the peaks is mainly due to rotation. The expression by Huang (1972),

$$R_e = \left(\frac{2\,V \sin i}{\Delta V_{\mathrm{peak}}}\right)^{\frac{1}{j}} R_\star,$$

leads to values around 2 $R_\star$ for $j = 1$ (conservation of angular momentum) and around 4 $R_\star$ for $j = 0.5$ (Keplerian rotation). The column densities calculated in the previous section indicate the presence of a high-density circumstellar envelope close to the central star. An ejection of material could have taken place quite recently. New spectra of EW Lac with the same signal-to-noise relation as the 2008 spectra are desirable for studying the evolution of the emitting regions of this star.

V923 Aql is a typical shell Be star that presents, by the time of our IR spectra, an Hα profile with increasing emission and strong V/R variations. Even though we do not count on a good time coverage of Hα for this star, an increase in the emission-line wings and the strengthening of the central absorption feature from 2006 to the present seems to exist, which is characteristic of the disk growth of late-type Be stars (Clark et al. 2003). However, our contemporaneous near-IR lines of this star do not evidence the presence of an optically thick envelope. A slow dissipation of the disk could have had an IR spectroscopic counterpart before the strengthening of Hα occurred. It would be interesting to obtain time-resolved IR and optical spectra of V923 Aql in order to study its disk evolution.

88 Her and BK Cam belong to group I: their near-IR emission lines indicate the presence of an optically thick region close to the central star at the time of our spectroscopy. In the case of BK Cam, the atom column densities found in the previous section suggest the presence of compact and dense Humphreys' line-forming regions. Moreover, both objects show strengthening Hα profiles at the epoch of our near-IR observations, which evidence the growth of the circumstellar disk. Both objects could have recently gone through mass ejection episodes.

5. CONCLUSIONS

We present a sample of new simultaneous *K*- and *L*-band spectra of Be stars obtained with Gemini/NIRI in observing bands 2 and 3 (the latter corresponding to allocation time for ranked programs in which the observing conditions are relaxed). These observations have proved to be useful to study the behavior of hydrogen emission lines. IR hydrogen line flux ratio diagrams let us estimate the optical thickness of the circumstellar envelope.

Time-resolved *K*- and *L*-band spectroscopy would allow us to study the origin and evolution of the envelope as well as to set constraints on the different models. Thus, we propose to make a long-term study of some of our targets. It is interesting to remark that the instrumental configuration we used allowed us to obtain

good quality IR observations and to take profit of Gemini band 3 observing time.

We thank the anonymous referee for many comments and suggestions that helped us to improve this manuscript. Part of this work was supported by the Agencia Nacional de Promoción Científica y Tecnológica with the grant BID 1728 OC/AR PICT 111.

REFERENCES

Antonello, E., Fracassini, M., Pasinetti, L. E., & Pastori, L. 1982, Ap&SS, 83, 381
Arias, M. L., Cidale, L., & Ringuelet, A. E. 2004, A&A, 417, 679
Ashok, N. M., & Banerjee, D. P. K. 2000, in ASP Conf. Ser. 214, The Be Phenomenon in Early-Type Stars, ed. M. A. Smith, H. F. Henrichs, & J. Fabregat (San Francisco, CA: ASP), 468
Ashok, N. M., Banerjee, D. P. K., Varricatt, W., & Kamath, U. S. 2006, MNRAS, 368, 592
Baker, J. G., & Menzel, D. H. 1938, ApJ, 88, 52
Banerjee, D. P. K., Janardhan, P., & Ashok, N. M. 2001, A&A, 380, L13
Clark, J. S., & Steele, I. A. 2000, A&AS, 141, 65
Clark, J. S., Tarasov, A. E., & Panko, E. A. 2003, A&A, 403, 239
Coté, J., & van Kerkwijk, M. H. 1993, A&A, 274, 870
de Wit, W. J., Lamers, H. J. G. L. M., Marquette, J. B., & Beaulieu, J. P. 2006, A&A, 456, 1027
Doazan, V., Harmanec, P., Koubský, P., Krpata, J., & Zdarsky, F. 1982, A&A, 115, 138
Dougherty, S. M., Waters, L. B. F. M., Burki, G., Coté, J., Cramer, N., van Kerkwijk, M. H., & Taylor, A. R. 1994, A&A, 290, 609
Fekel, F. C. 1997, PASP, 109, 514
Floquet, M., et al. 2000, A&A, 362, 1020
Floquet, M., et al. 2002, A&A, 394, 137
Frémat, Y., Zorec, J., Hubert, A.-M., & Floquet, M. 2005, A&A, 440, 305
Gehrz, R. D., Hackwell, J. A., & Jones, T. W. 1974, ApJ, 191, 675
Grady, C. A., Sonneborn, G., Wu, C.-C., & Henrichs, H. F. 1987, ApJS, 65, 673
Granada, A., & Cidale, L. S. 2006, RevMexAA (Serie de Conferencias), 26, 172
Hamann, F., & Simon, M. 1987, ApJ, 318, 356
Hanson, M. M., Conti, P. S., & Rieke, M. J. 1996, ApJS, 107, 281
Hanuschik, R. W. 1989, Ap&SS, 161, 61
Harmanec, P., Koubský, P., & Krpata, J. 1972, Bull. Astron. Inst. Czech., 23, 218
Hirata, R. 1995, PASJ, 47, 195
Hirata, R. 2007, in ASP Conf. Ser. 361, Active OB Stars: Laboratories for Stellar and Circumstellar Physics, ed. S. Štefl, P. Owocki, & A. T. Okazaki (San Francisco, CA: ASP), 267
Hony, S., et al. 2000, A&A, 355, 187
Huang, S. S. 1972, ApJ, 171, 549
Hummel, W. 1998, A&A, 330, 243
Hummel, W., & Dachs, J. 1992, A&A, 262, L17
Hummel, W., & Vrancken, M. 2000, A&A, 359, 1075
Jaschek, C., & Jaschek, M. 1987, The Classification of Stars (Cambridge: Cambridge Univ. Press)
Jeong, J. H., Suh, C. W., & Nha, I.-S. 1986, Ap&SS, 119, 73
Katahira, J.-I., Hirata, R., Ito, M., Katoh, M., Ballereau, D., & Chauville, J. 1996, PASJ, 48, 317
Koubský, P., Harmanec, P., Gulliver, A. F., Ballereau, D., & Chauville, J. 1989, Bull. Astron. Inst. Czech., 40, 31
Lenorzer, A., de Koter, A., & Waters, L. B. F. M. 2002a, A&A, 386, L5
Lenorzer, A., Vandenbussche, B., Morris, P., de Koter, A., Geballe, T. R., Waters, L. B. F. M., Hony, S., & Kaper, L. 2002b, A&A, 384, 473
Lynch, D. K., Rudy, R. J., Mazuk, S., & Puetter, R. C. 2000, ApJ, 541, 791
Lynch, D. K., Rudy, R. J., Venturini, C. C., Mazuk, S., & Puetter, R. C. 2001, AJ, 122, 2013
Lynds, C. R. 1960, ApJ, 131, 390
Mason, B. D., Hartkopf, W. I., Gies, D. R., Henry, T. J., & Helsel, J. W. 2009, AJ, 137, 3358
McLaughlin, D. B. 1963, ApJ, 137, 1085
Mennickent, R. E., Sabogal, B., Granada, A., & Cidale, L. 2009, PASP, 121, 125
Mennickent, R. E., Vogt, N., & Sterken, C. 1994, A&AS, 108, 237
Merrill, P. W. 1952, ApJ, 116, 501
Osterbrock, D. E. 1989, Astrophysics of Gaseous Nebulae and Active Galactic Nuclei (Mill Valley, CA: Univ. Science Books)
Pavlovski, K., Harmanec, P., Božić, H., Koubský, P., Hadrava, P., Kříž, S., Ružić, Ž., & Štefl, S. 1997, A&AS, 125, 75
Pavlovski, K., Ružić, Ž., Pavlović, M., Jeong, J. H., & Nha, I.-S. 1993, Ap&SS, 200, 201
Percy, J. R., & Bakos, A. G. 2001, PASP, 113, 748
Percy, J. R., Desjardins, A., & Yeung, D. 1996, J. Am. Assoc. Var. Star Obs., 25, 14
Persson, S. E., & McGregor, P. J. 1985, AJ, 90, 1860
Peters, G. J. 1988, PASP, 100, 207
Peters, G. J. 2000, in ASP Conf. Ser. 214, The Be Phenomenon in Early-Type Stars, ed. M. A. Smith, H. F. Henrichs, & J. Fabregat (San Francisco, CA: ASP), 212
Peters, G. J., & Penrod, G. D. 1988, in A Decade of UV Astronomy with IUE Satellite, Vol. 2, ed. N. Longdon & E. J. Rolfe (ESA SP-281b; Noordwijk: ESA), 117
Reig, P., Negueruela, I., Fabregat, J., Chato, R., & Coe, M. J. 2005, A&A, 440, 1079
Rieke, G. H., & Lebofsky, M. J. 1985, ApJ, 288, 618
Royer, F., Zorec, J., & Gómez, A. E. 2007, A&A, 463, 671
Sadakane, K., Hirata, R., & Tsuji, T. 2005, PASJ, 57, 1
Slettebak, A. 1982, ApJS, 50, 55
Steele, I. A., & Clark, J. S. 2001, A&A, 371, 643
Štefl, S., Baade, D., Rivinius, Th., Otero, S., Stahl, O., Budovičová, A., Kaufer, A., & Maintz, M. 2003, A&A, 402, 253
Štefl, S., Hadrava, P., Baade, D., Rivinius, Th., Maintz, M., & Stahl, O. 2004, in IAU Symp. 215, Stellar Rotation, ed. A. Maeder & P. Eenens (San Francisco, CA: ASP), 166
Tanaka, K., Sadakane, K., Narusawa, S.-Y., Naito, H., Kambe, E., Katahira, J.-I., & Hirata, R. 2007, PASJ, 59, L35
Taranova, O., Shenavrin, V., & Nadjip, A. D. 2008, Perem. Zvezdy Prilozhenie, 8, 6
Tubbesing, S., Rivinius, Th., Wolf, B., & Kaufer, A. 2000, in ASP Conf. Ser. 214, The Be Phenomenon in Early-Type Stars, ed. M. A. Smith, H. F. Henrichs, & J. Fabregat (San Francisco, CA: ASP), 232
Walker, M. F. 1958, AJ, 63, 237
Waters, L. B. F. M., Coté, J., & Lamers, H. J. G. L. M. 1987, A&A, 185, 206
Zorec, J., Arias, M. L., Cidale, L., & Ringuelet, A. E. 2007, A&A, 470, 239